A Novel Motion Artifact Detection Algorithm Based on Recurrence Plot Processing of Photoplethysmogram Signal

S. M. A. Salehizadeh
Department of Biomedical Engineering
University of Connecticut
Storrs, CT, USA
smasalehizadeh@gmail.com

Ki H. Chon
Department of Biomedical Engineering
University of Connecticut
Storrs, CT, USA
ki.chon@uconn.edu

***Abstract*—In this study, we propose a novel procedure "RepMA" based on image processing of recurrence plots to detect motion artifacts (MA) in PPG signals. The idea is by using recurrence plots we convert the signal into a binary image that can be processed later for distortion and corruption. The algorithm runs on each 4 sec segments of the signal and the recurrence plot (image) of each segment is then preprocessed and analyzed to determine if the segment is clean or corrupted by noise. The MAs change the signal recurrence behavior and their irregular recurrence patterns that can be utilized to distinguish between clean and corrupted PPG segment. We used the lab controlled PPG recordings from forehead and finger pulse oximeter sensors with random movements for evaluating of RepMA performance. The results of RepMA algorithm were compared to two different algorithms known for their alleged competency in MA detection: the Hjorth and Shannon entropy. The proposed detection method outperforms the two other methods in terms of accuracy, run-time, specificity and sensitivity. Moreover, our algorithm is able to be implemented in real-time.**

Keywords—motion artifact, pulse oximeter, photoplethysmogram, recurrence plot, image processing

I. INTRODUCTION

PULSE oximeter (PO) is a non-invasive, low cost device that is widely used in hospitals and clinics to monitor heart rate (HR) and arterial oxygen saturation (SpO2). However, extraction of the above mentioned vital signs and other physiological parameters using PO is predicated on artifact-free PPG data. It is well known that PPG is highly sensitive to artifacts, particularly those generated while the patient is in motion [1, 2]. This imposes a huge limitation on the usability of the PPG for ambulatory monitoring applications. Motion and noise artifacts (MAs) distorting PPG recordings can cause erroneous estimation of HR and SpO2 [2, 3]. Although there are techniques which have been proposed to alleviate the effects of MAs, solution to this problem still remains unsatisfactory in practice. Several algorithm-based MA reduction methods were proposed, such as time and frequency domain filtering, power spectrum analysis, and blind source separation techniques [2, 4]. These techniques reconstruct noise contaminated PPG such that a noise-reduced signal is obtained. However, the reconstructed signal typically contains incomplete dynamic features of the uncorrupted PPG and some algorithms are solely designed to capture only the HR and SpO_2 information instead of the signal's morphology and its amplitudes, which are needed for other physiological derivations [5]. MA detection methods are mostly based on a signal quality index (SQI) which quantifies the severity of the artifacts. Some approaches quantify the SQI using waveform morphologies [1, 6] or filtered output [7, 8] , while other derive the SQI with the help of additional hardware such as accelerometer and electrocardiogram [9]. Statistical measures, such as skewness, kurtosis (K), and quadratic phase coupling [10], Shannon entropy (SE), and Renyi's entropy [11], have been shown to be helpful in determining the SQI. These statistical algorithms discriminate amplitude distributions between PPG segments with an assumption that clean and corrupt segments would form two separate groups. However, PPG morphology vary among patients, thus yielding multitude of amplitude distributions. Therefore, it would be difficult to obtain high accuracy from these algorithms in practice. In this paper, a new real-time algorithm based on recurrence quantification is presented that can distinguish between PPG signal with motion and noise artifacts and MA-free signals. The idea is to process the PPG signal in time-time domain by transforming the 1-D signal to a 2-D image and analyze the image for MA detection. The algorithm comprised of 5 distinct stages and it is called "RepMA": (1) Downsampling, (2) Transforming 1-D PPG vector to time-time Recurrence 2-D plots (3) Image processing, (4) MA detection.

II. EXPERIMENTS

A. Databases

The RepMA algorithm was evaluated on two different datasets. The data were recorded in controlled condition from 10 subjects in Chon lab. For the laboratory controlled environment, both forehead and finger worn PO sensor data were collected from healthy subjects recruited from the student community of the University of Connecticut (UConn). The study was approved by UConn's IURB and all subjects' informed consents were collected prior to data

recordings. Laboratory data allows us to have more control over the duration of MNA generated to ensure that the detection phase of algorithm was tested on a wide range of MNA duration. In laboratory-controlled head and finger movement data, motion artifacts were induced by head and finger movements for specific time intervals in both horizontal and vertical directions. For head movement data, 10 healthy volunteers were asked to wear our PO on the forehead along with a reference Masimo Radical (Masimo SET®) finger type transmittance pulse oximeter. The subjects were all healthy with no past histories of cardiovascular diseases. After baseline recording for 5 minutes without any movement, subjects were instructed to introduce motion artifacts for specific time intervals varying from 10 to 50% within a 1 minute segment. For example, if a subject was instructed to perform left-right random movements for 6 seconds, a 1 min segment of data would contain 10% noise. The finger laboratory movement data were recorded in a similar setup as the head data using our custom-made PPG finger sensor.

B. Pre-processing of PPG data

US Army Medical Research and Materiel Command (USAMRMC) under Grant No. W81XWH-12-1-0541All PPG data were pre-processed by a 6th order infinite impulse response (IIR) band pass filter with cut-off frequencies of 0.1 Hz and 10 Hz. Zero-phase forward and reverse filtering was applied to account for the non-linear phase of the IIR filter. Many recent publications on MNA detection utilized human visual inspection from experts who were familiar with PPG and their decisions are regard it as the gold standard for marking MNA corrupted data [1, 11]. In our work, we also use the human visual inspection to establish a MNA reference for our datasets. Three inspectors individually marked MNA corrupted portions of the PPG. Disagreements of the marked portions were resolved by majority votes.

III. METHODS

Noise depending on the level, can distort any existing structure in a recurrence plot [12, 13]. It is desirable that the smallest distance threshold be chosen to increase the resolution of the time-time 2D recurrence plot (RP) image. However, higher distance threshold value preserves the distortions that are produced by movement and noise artifacts. The embedding dimension on the other hand has to be chosen so that the dynamics of the system will be well presented by its phase space dynamics. Movement during PPG recordings can increase moiton artifacts by introducing irregular sudden peaks in the recordings which produce more continuous vertical and/orhorizontal patterns (see 4th panel of Fig. 1). Motion and noise artifact detection procedure of the RepMA algorithm is presented in Table (1).

Table (1) RepMA Algorithm Steps

Step 1. Down-sampling PPG signal
- In order to reduce the complexity and run-time the PPG segment at each window is resampled to ¼ of its original sampling frequency.

Step 2. Convert from 1-D PPG vector to 2-D time-time recurrence image
- At this step recurrence matrix is calculated using the Eq.3 for original PPG for each 4 sec window segment.

Step 3. Recurrence Image Processing
- The recurrence image in this step is preprocessed to distinguish between image of a clean PPG versus MA corrupted.

Step 4. Motion artifact detection
- Results from of step 3 are compared to a reference threshold values to specify if a PPG segment is clean or corrupted.

Recurrence analysis is a graphical method designed to unwrap hidden recurring nonstationary patterns and structural changes in signals [12, 13]. Recurrence is a fundamental property of dynamical systems, which can be exploited to characterize the system's behavior in phase space. Recurrence occurs when a dynamical system returns to former states. The common recurrence plot is usually defined according to a neighborhood criterion and a threshold distance ε, by which the paired distances smaller than the threshold assigned with 1 and the rest with 0. Such an RP can be mathematically expressed as

$$RP_{ij}^{m} = \Theta\left(\varepsilon_i - \left\|\vec{x}_i - \vec{x}_j\right\|\right), \quad \vec{x}_i \in \mathbb{R}^m, \quad i, j = 1,2,\ldots,N \qquad (4)$$

where $\|.\|$ is a norm and $\Theta(.)$ is the Heaviside function.

Recurrence Image Processing

Table (2) presents the step-by-step recurrence image processing procedure of RepMA algorithm. The top two panels of Fig. 1 show a 4 sec of a clean PPG and MA-corrupted PPG segments, respectively, and their corresponding recurrence plots are shown in the bottom panels. To discriminate between the clean and corrupted PPG signal using the recurrence plots, we summarize the RepMA procedures.

Table (2) Recurrence Image Processing Procedure in RepMA Algorithm

Stage 1. Calculate the recurrence image for each 4 sec PPG segment data
1.1. Save a reference clean image of PPG
1.2. Update clean reference when a new clean segment is detected

Stage 2. Remove objects attached to the sides of recurrence image

Stage 3. Extract separate objects from the results of Step 2.

Stage 4. Objects alignment with reference by rescaling and rotation

Stage 5. Calculate the MA corruption criteria of objects from Step 4 using the image centroid equations

$$M_{ij} = \sum_{x}\sum_{y} x^i\, y^i RI(x,y)$$

$$Centriod(x)_{Obj(k)} = \frac{M_{10}}{M_{00}},\quad Centriod(y)_{obj(k)} = \frac{M_{01}}{M_{00}}$$

$$MAcr_{image(i)}(k) = \left|Centriod(x)_{Ref\_Object} - Centriod(x)_{Obj(k)}\right| \times \left|Centriod(x)_{Ref\_Object} - Centriod(x)_{Obj(k)}\right|$$

where $k = 1,2,\dots,K(\#objects\ in\ the\ image)$ and $i = 1,2,\dots,N$, is i^{th} PPG segment of 4 sec.

Step 6. Set the threshold for motion artifact detection as

$$Thd = 5\% \times Centriod(x)_{Ref\_Object} \times Centriod(y)_{Ref\_Object}$$

By comparing the $MAcr(k)$ for each object (k) to the defined threshold, if $\max(MAcr_{image(i)}) > Thd$, then the object (k) in the recurrence image of the corresponding 4-sec segment PPG is corrupted by motion and in total the segment labeled as corrupted. Otherwise if the criteria for all objects in the recurrence image fall below the threshold then the entire image belongs to a clean PPG segment. At this step recurrence matrix is calculated using the Eq.3 for original PPG for each 4 sec window segment.

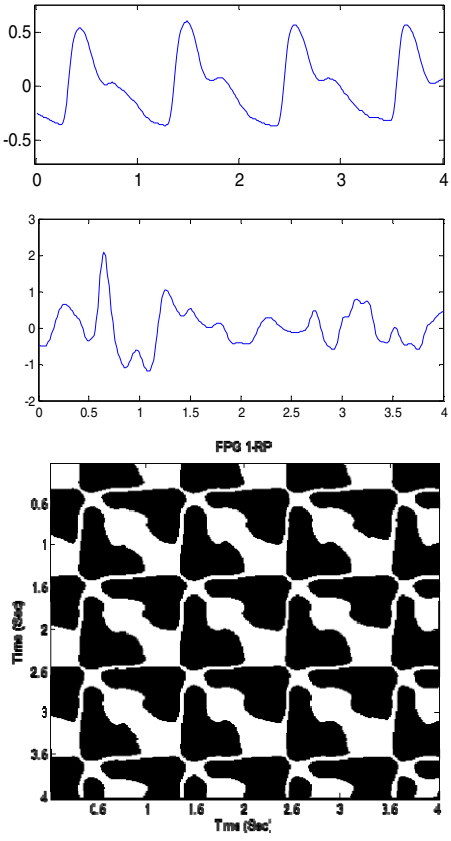

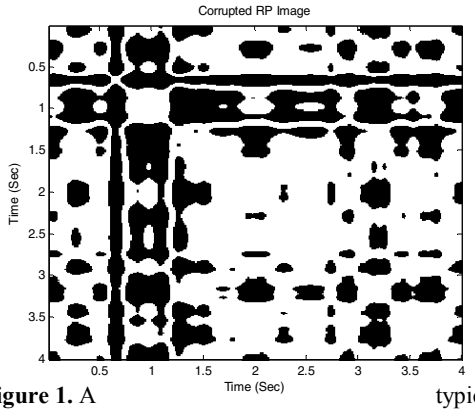

Figure 1. A typical clean vs. corrupted PPG segment. **(1st row)** Clean 4 sec PPG, **(2nd row)** MA Corrupted PPG, **(3rd row)** Clean Recurrence Image **(4th row)** Corrupted Recurrence Image

Fig. 2 illustrate the results after removing the objects from the left diagonal recurrence image of both clean and corrupted segments. After removing edge objects, third step is to extract all of the separate objects remain in the image.

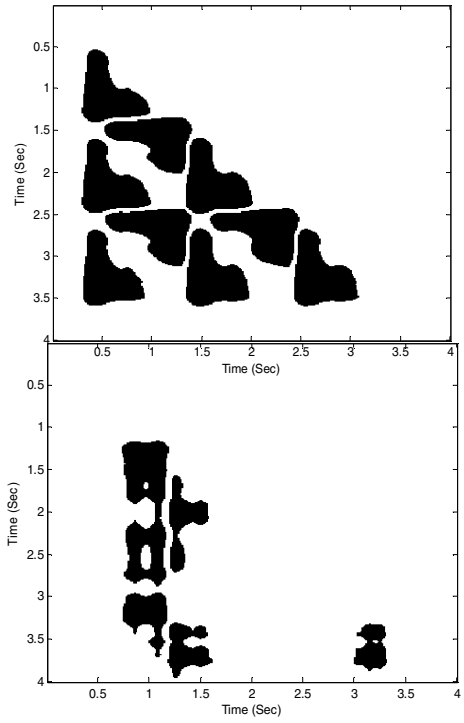

Figure 2. Removing edge objects from left-diagonal recurrence image: **(top panel)** Clean Image, **(bottom panel)** Corrupted Image

Fig. 3 represents the RepMA detection results when compared to reference MA detection index of the whole recordings #3. It can be seen that RepMA successfully detect the MA corrupted segments of PPG. In the next section, results of RepMA on two datasets in comparison to two other MA detection methods (Hjorth and Shannon entropy) are presented.

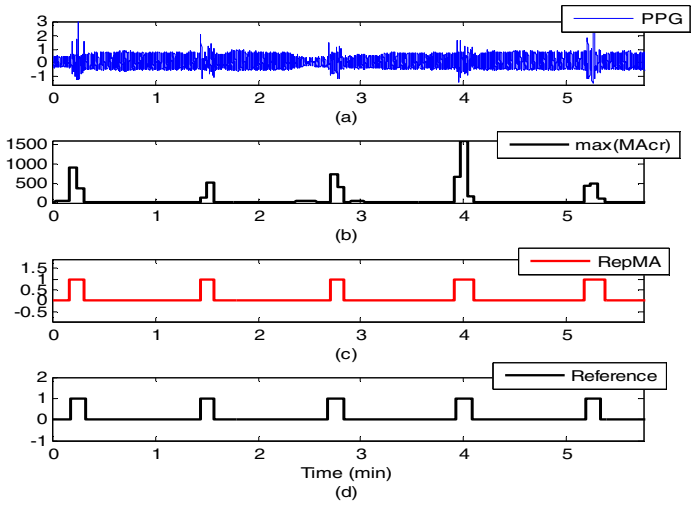

Figure 3. Subject#3. **(a)** PPG signal. **(b)** RepMA detection signal, **(c)** max of $MAcr$ signal, **(d)** Reference detection signal

IV. RESULTS

We present the performance of RepMA algorithm using both forehead and finger datasets. Detection performance was evaluated by comparing results of RepMA and the two other MA detection algorithms to the MNA reference (as determined visually by the experts) to obtain accuracy, sensitivity, and specificity. For the forehead PPG recordings, the accuracy, sensitivity and specificity values of the RepMA were found to be 96.8%, 96.3% and 97.5%, respectively. For Hjorth's approach, the accuracy, sensitivity and specificity values were found to be 72.5%, 47.2% and 84.4%, respectively. For Shannon entropy's approach, the accuracy, sensitivity and specificity values were found to be 83.1%, 56.6% and 91.5%, respectively.

For the finger PPG recordings, the accuracy, sensitivity and specificity values of the RepMA were found to be 97.8%, 94.1% and 98.3%, respectively. For Hjorth's approach, the accuracy, sensitivity and specificity values were found to be 91.1%, 83.5% and 96.2%, respectively. For Shannon entropy's approach, the accuracy, sensitivity and specificity values were found to be 58.5%, 34.6% and 86.3%, respectively.

It can be observed from these results that RepMA algorithm's accuracy, sensitivity and specificity values are significantly higher than the other two methods on average over all recordings from the forehead and finger datasets.

V. DISCUSSION & CONCLUSION

In this study, we propose a novel MA detection (RepMA) that is based on recurrence image processing. The idea is to transform the one dimensional PPG data into a 2 dimensional image using recurrence plot quantification. The main point is MA corrupted data is easier to be detected when we look into the recurrence features of PPG in its recurrence plot. We showed that RepMA can provide more accurate results on both lab-controlled datasets when compared to two other MA detection method: (1) Hjorth [14] and (2) Shannon Entropy [11]. Moreover, the accuracy, sensitivity and specificity values on average of our proposed method were significantly higher than other methods).

ACKNOWLEDGMENT

This work was supported in part by the US Army Medical Research and Materiel Command (USAMRMC) under Grant No. W81XWH-12-1-0541.

REFERENCES

[1] J. W. Chong *et al.*, "Photoplethysmograph signal reconstruction based on a novel hybrid motion artifact detection-reduction approach. Part I: Motion and noise artifact detection," *Ann Biomed Eng,* vol. 42, no. 11, pp. 2238-50, Nov 2014.

[2] S. M. Salehizadeh *et al.*, "Photoplethysmograph signal reconstruction based on a novel motion artifact detection-reduction approach. Part II: Motion and noise artifact removal," *Ann Biomed Eng,* vol. 42, no. 11, pp. 2251-63, Nov 2014.

[3] J. harvey, S. M. Salehizadeh, Y. Mendelson, and K. H. Chon, "OxiMA: A new approach to address motion artifact in photoplethysmogram signals for ac-curate estimation of hypoxia and pulse rates using signal frequency component analysis," *IEEE Trans Biomed Eng,* 2018.

[4] T. L. Rusch, R. Sankar, and J. E. Scharf, "Signal processing methods for pulse oximetry," *Comput Biol Med,* vol. 26, no. 2, pp. 143-59, Mar 1996.

[5] S. M. Salehizadeh, D. Dao, J. Bolkhovsky, C. Cho, Y. Mendelson, and K. H. Chon, "A Novel Time-Varying Spectral Filtering Algorithm for Reconstruction of Motion Artifact Corrupted Heart Rate Signals During Intense Physical Activities Using a Wearable Photoplethysmogram Sensor," *Sensors (Basel),* vol. 16, no. 1, Dec 23 2015.

[6] D. Dao *et al.*, "A Robust Motion Artifact Detection Algorithm for Accurate Detection of Heart Rates From Photoplethysmographic Signals Using Time-Frequency Spectral Features," *IEEE J Biomed Health Inform,* vol. 21, no. 5, pp. 1242-1253, Sep 2017.

[7] W. Karlen, K. Kobayashi, J. M. Ansermino, and G. A. Dumont, "Photoplethysmogram signal quality estimation using repeated Gaussian filters and

cross-correlation," *Physiol Meas,* vol. 33, no. 10, pp. 1617-29, Oct 2012.

[8] S. S. a. L. Seyedtabaii, "Kalman filter based adaptive reduction of motion artifact from photoplethysmographic signal," *World Academy of Science, Engineering and Technology,* vol. 37, 2008.

[9] J. Y. Foo and S. J. Wilson, "A computational system to optimise noise rejection in photoplethysmography signals during motion or poor perfusion states," *Med Biol Eng Comput,* vol. 44, no. 1-2, pp. 140-5, Mar 2006.

[10] R. Krishnan, B. B. Natarajan, and S. Warren, "Two-stage approach for detection and reduction of motion artifacts in photoplethysmographic data," *IEEE Trans Biomed Eng,* vol. 57, no. 8, pp. 1867-76, Aug 2010.

[11] N. Selvaraj, Y. Mendelson, K. H. Shelley, D. G. Silverman, and K. H. Chon, "Statistical approach for the detection of motion/noise artifacts in Photoplethysmogram," *Conf Proc IEEE Eng Med Biol Soc,* vol. 2011, pp. 4972-5, 2011.

[12] D. Auerbach, P. Cvitanovic, J. P. Eckmann, G. Gunaratne, and I. I. Procaccia, "Exploring chaotic motion through periodic orbits," *Phys Rev Lett,* vol. 58, no. 23, pp. 2387-2389, Jun 8 1987.

[13] R. Bakker, J. C. Schouten, C. L. Giles, F. Takens, and C. M. van den Bleek, "Learning chaotic attractors by neural networks," *Neural Comput,* vol. 12, no. 10, pp. 2355-83, Oct 2000.

[14] B. Hjorth, "The physical significance of time domain descriptors in EEG analysis," *Electroencephalogr Clin Neurophysiol,* vol. 34, no. 3, pp. 321-5, Mar 1973.